SUPPORTING INFORMATION

Study of the Influence of Magnetic Dilution over Relaxation Processes in a Zn/Dy Single-Ion Magnet by Correlation between Luminescence and Magnetism

Jérôme Long,*[a] Ekaterina Mamontova,[a] Vania Freitas,[b] Dominique Luneau,[c] Vaecheslav Vieru,[d] Liviu F. Chibotaru,[d] Rute A. S. Ferreira,[b] Gautier Félix,[a] Yannick Guari,[a] Luis D. Carlos[b] and Joulia Larionova[a]

[a] *Institut Charles Gerhardt Montpellier, UMR 5253, Ingénierie Moléculaire et Nano-Objets, Université de Montpellier, ENSCM, CNRS, Place E. Bataillon, 34095 Montpellier Cedex 5 (France).*

[b] *Physics Department and CICECO – Aveiro Institute of Materials, University of Aveiro, 3810-193, Aveiro (Portugal).*

[c] *Laboratoire des Multimatériaux et Interfaces (UMR 5616), Université Claude Bernard Lyon 1, Campus de la Doua, 69622 Cedex Villeurbanne (France).*

[d] *Theory of Nanomaterials Group and INPAC, Katholieke Universiteit Leuven, Celesijnenlaan, 200F, Heverlee, B-3001(Belgium).*

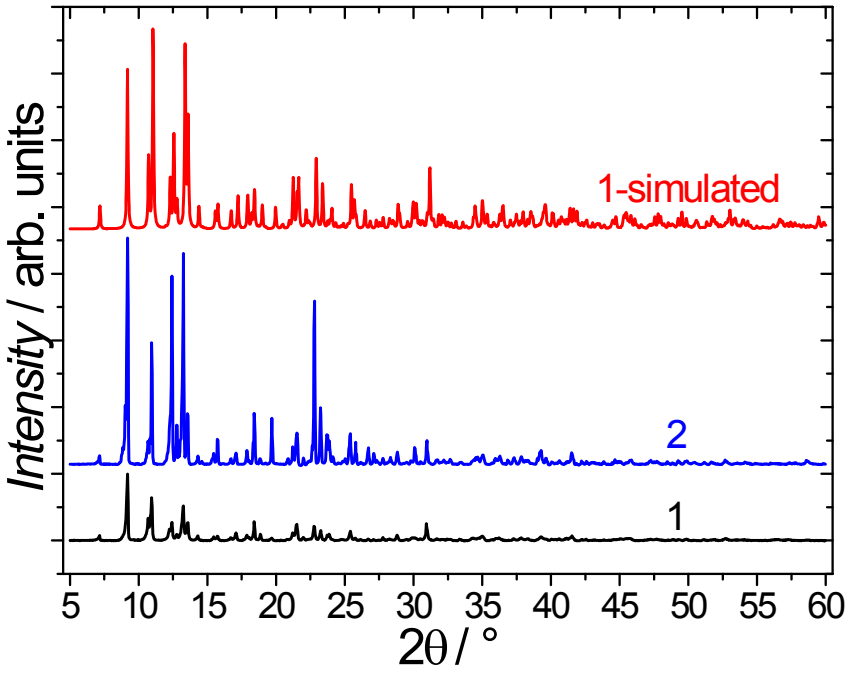

Figure S1: PXRD patterns for 1, 2. The red line accounts for the simulated pattern for 1 from the single crystal -X Ray diffraction.

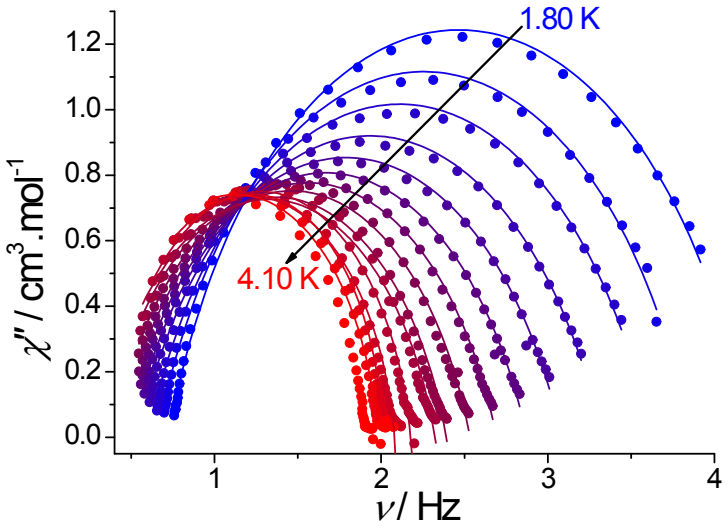

Figure S2: Cole-Cole (Argand) plot obtained using the ac susceptibility data (900 Oe) for **1**. The solid lines correspond to the best fit obtained with a generalized Debye model.

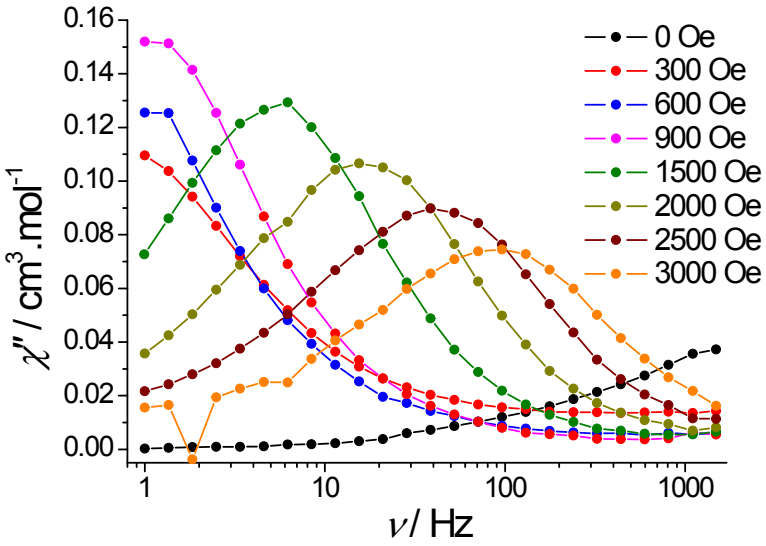

Figure S3. Frequency dependence of χ'' as a function of the applied dc field at 1.8 K for **2.** Line is a guide for the eyes.

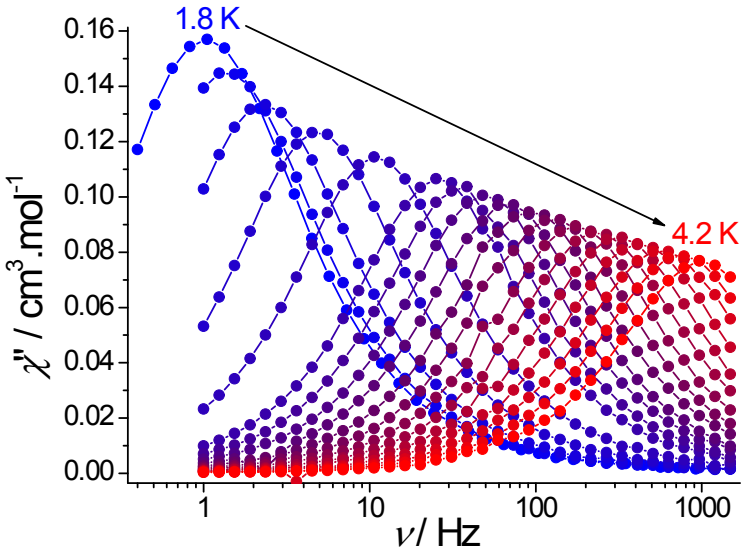

Figure S4. Frequency dependence of χ'' for **2** under a 900 Oe DC field**.** Line is a guide for the eyes.

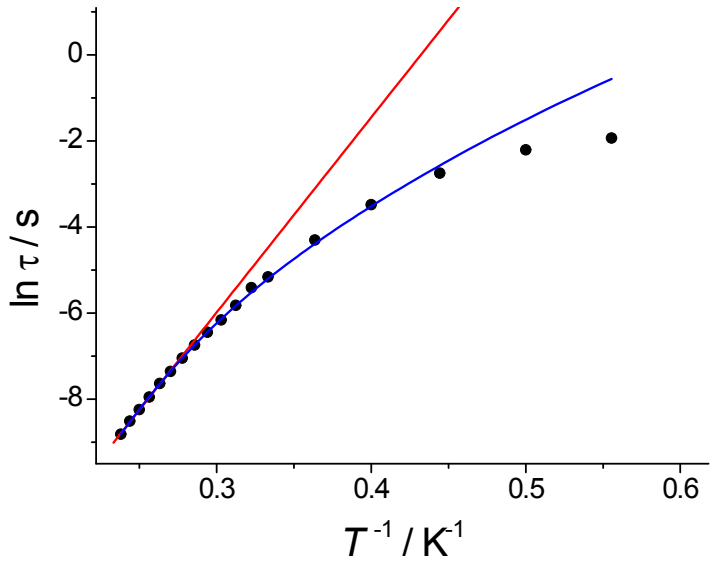

Figure S5. Temperature dependence of the relaxation time for **2** under a 900 Oe DC field**.** The red solid line represents the Arrhenius fit while the blue solid lines accounts for the fit using Eq. 2.

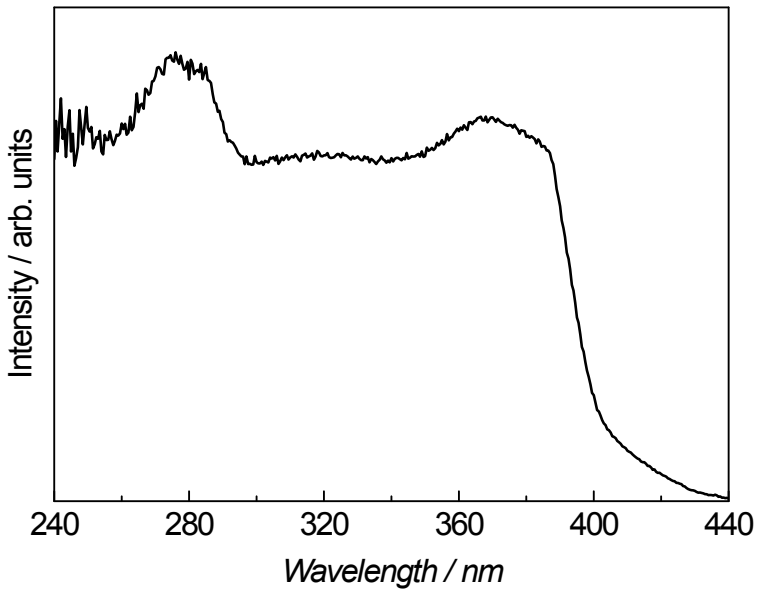

Figure S6. Excitation spectrum acquired at 14 K for **2** monitored at 478 nm.

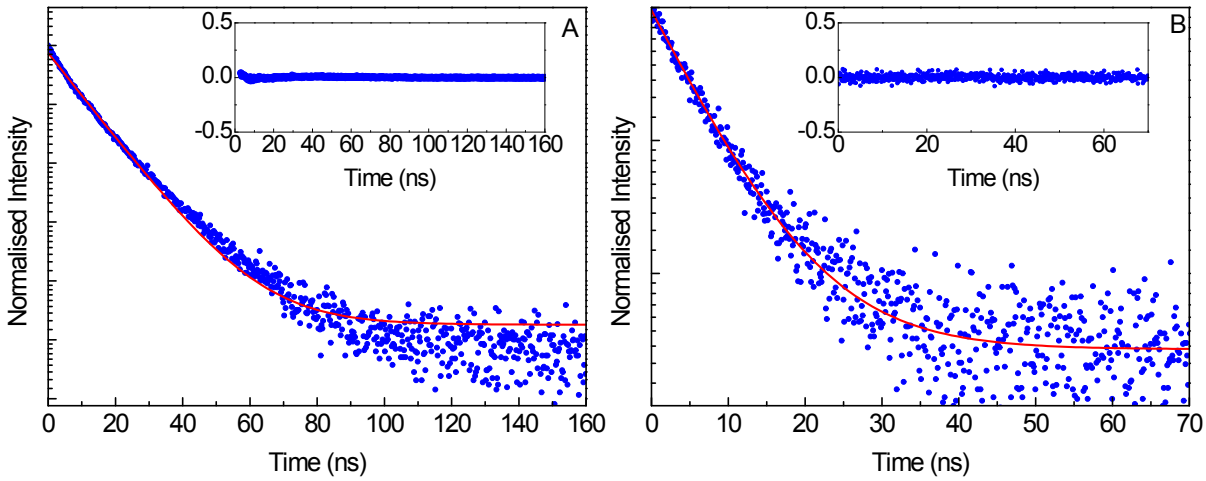

Figure S7. Low-temperature (12 K) emission decay curves for (A) **1** and (B) **2** monitored at 478 nm and excited at 390 nm. The solid lines represent the data best fit (R^2>0.99) using a single exponential function and the insets show the fit regular residual plot.

Table S1. Crystal and structure refinement data for compounds **1** and **2**.

	1	**2**
Formula	$C_{18}H_{20}N_5O_{14}ZnDy$	$C_{18}H_{20}N_5O_{14}ZnY$*
Formula weight	758.26	685.69
Temperature / K	173(2)	293(2)
Crystal system	Monoclinic	Monoclinic
Space group	$P2_1/n$	$P2_1/n$
a/Å	7.75620(16)	7.8023(3)
b/Å	19.2440(4)	19.2183(8)
c/Å	16.0150(3)	16.1293(6)
β/º	91.3111(18)	91.994(4)
Volume/Å^3	2389.79(8)	2417.07(16)
Z	4	4
D_c/g cm^{-3}	2.108	1.8962
μ(Mo-Kα)/mm^{-1}	4.190	3.582
F(000)	1484	1568
Crystal size/mm	0.22×0.10×0.02	0.40×0.35×0.10
Crystal type	Colourless plates	Colourless plates
θ range	3.59 to 29.13	2.74 to 29.31
Index ranges	$-10 \le h \le 10$	$-10 \le h \le 7$
	$-26 \le k \le 26$	$-25 \le k \le 21$
	$-21 \le l \le 21$	$-20 \le l \le 21$
Reflections collected	41024	14130
Independent reflections	6424 (R_{int} = 0.0288)	5697 (R_{int} = 0.0263)
Data completeness	99.8%	99.8%
Data / parameters	6424 / 360	5697 / 256
Final R indices [I>2σ(I)][a,b]	$R1$ = 0.0163	$R1$ = 0.0368
	$wR2$ = 0.0339	$wR2$ = 0.0982
Final R indices (all data)[a,b]	$R1$ = 0.0201	$R1$ = 0.0474
	$wR2$ = 0.0348	$wR2$ = 0.0982
Largest diff. peak and hole	0.418 and -0.370 eÅ^{-3}	0.75 and -0.66 eÅ^{-3}

[a] $R1 = \sum \| F_o | - | F_c \| / \sum | F_o |$; [b] $wR2 = \sqrt{\sum \left[w \left(F_o^2 - F_c^2 \right)^2 \right] / \sum \left[w \left(F_o^2 \right)^2 \right]}$

***** The Dy ions cannot be experimentally assigned in the crystal structure.

Table S2. SHAPE analysis for compounds **1** and **2**.

	JJCU	CCU	JCSAPR	CSAPR	JTCTPR	TCTPR
1	8.990	7.201	3.965	2.611	4.275	2.543
2	9.231	7.418	4.109	2.727	4.275	2.503

JJCU:Capped cube
CCU: Spherical-relaxed capped cube
JCSAPR: Capped square antiprism
CSAPR: Spherical capped square antiprism
JTCTPR: Tricapped trigonal prism
TCTPR: Spherical tricapped trigonal prism

Table S3. Fit parameters of the field dependence of the relaxation time obtained using the Eq. 1

Compound	D ($s^{-1}K^{-1}Oe^{-4}$)	B_1 (s^{-1})	B_2 (Oe^{-2})
1	1.231×10^{-11}	374.11	5.05×10^{-6}
2	6.661×10^{-12}	8.76	8.00×10^{-6}

Table S4. Fitting of the Cole-Cole plots with a generalized Debye model for temperature ranging from 1.8 to 4.1 K under a 900 Oe DC field for **1**.

T (K)	α	χ_S ($cm^3. mol^{-1}$)	χ_T ($cm^3. mol^{-1}$)
1.8	0.265	1.111	3.818
2.0	0.288	1.041	3.471
2.2	0.323	1.007	3.214
2.4	0.342	0.937	3.928
2.6	0.3444	0.866	2.712
2.8	0.329	0.791	2.541
3.0	0.302	0.716	2.406
3.2	0.278	0.644	2.282
3.4	0.258	0.573	2.168
3.5	0.248	0.533	2.113
3.7	0.128	0.483	2.074
3.9	0.116	0.434	1.990
4.0	0.032	0.476	1.985

4.1	0.096	0.351	1.906

Table S5. Fitting of the Cole-Cole plots with a generalized Debye model for temperature ranging from 1.8 to 4.2 K under a 600 Oe DC field for **2**.

T (K)	α	χ_S (cm^3. mol^{-1})	χ_T (cm^3. mol^{-1})
1.8	0.413	0.12	0.515
2.0	0.362	0.0866	0.417
2.2	0.126	0.039	0.31
2.4	0.186	0.0367	0.284
2.6	0.093	0.026	0.26
2.8	0.0855	0.0228	0.243
3.0	0.0617	0.0185	0.226
3.1	0.033	0.0171	0.22
3.2	0.055	0.017	0.212
3.3	0.0365	0.01497	0.207
3.4	0.0319	0.0139	0.201
3.5	0.02388	0.037	0.197
3.6	0.0338	0.0135	0.191
3.7	0.0177	0.0126	0.187
3.8	0.0131	0.0119	0.182
3.9	0.00322	0.01309	0.179
4.0	2.5E-5	0.0126	0.175
4.1	0.00207	0.0147	0.17
4.2	0.108	0	0.159
4.3	2.56E-4	0.014	0.163

Table S6. Fit parameters of the temperature dependence of the relaxation time for 2 obtained using Eq. 2 (900 Oe dat).

Compound	Δ (cm^{-1})	τ_0 (s)	C_{raman} (s^{-1}.K^{-9})	A (s^{-1}.K^{-1})
2 (900 Oe)	44 ± 2	(9.8 ± 0.5) × 10^{-11}	0.0088 ± 0.0004	0
2 (900 Oe)	52 *	(7.1 ± 0.2) × 10^{-12}	0.0102 ± 0.0002	0

** fixed from photoluminescence*

Table S7. Contractions of the employed basis sets in computational approximations **1** and **2**.

Basis 1	**Basis 2**
Dy.ANO-RCC...7s6p4d2f1g. Zn.ANO-RCC...5s4p2d1f. N.ANO-RCC...3s2p1d. O.ANO-RCC...3s2p1d. C.ANO-RCC...3s2p. H.ANO-RCC...2s.	Dy.ANO-RCC...8s7p5d3f2g1h. Zn.ANO-RCC...6s5p3d2f1g. N.ANO-RCC...4s3p2d1f. (close) N.ANO-RCC...3s2p. (distant) O.ANO-RCC...4s3p2d1f. (close) O.ANO-RCC...3s2p. (distant) C.ANO-RCC...4s3p2d. (close) C.ANO-RCC...3s2p. (distant) H.ANO-RCC...3s2p1d. (close) H.ANO-RCC...2s. (distant)

Table S8. Energies of the lowest Kramers doublets (cm^{-1}) of Dy center for **1**.

Dy_basis1 X-ray structure	Dy_basis2 X-ray structure	Dy_basis1 Hydrogens-optimized	Dy_basis2 Hydrogens-optimized	Dy_basis1 Entire complex optimized	Dy_basis2 Entire complex optimized
0	0	0	0	0	0
68	73	61	66	59	59
126	146	120	137	84	89
154	187	153	188	97	128
177	214	171	209	147	176
238	271	229	263	196	225
286	316	276	310	278	319
309	375	305	368	316	347

Table S9. The *g* tensors of the lowest Kramers doublets (KD) of Dy center.

KD	**Dy_basis1 X-ray structure**	**Dy_basis2 X-ray structure**	**Dy_basis1 H-optmized**	**Dy_basis2 H-optmized**	**Dy_basis1 Entire complex optimized**	**Dy_basis2 Entire complex optimized**

		g	*g*	*g*	*g*	*g*	*g*
1	g_X	0.032724	0.075290	0.085899	0.099417	0.092613	0.201081
	g_Y	0.173381	0.221671	0.260023	0.283988	0.145213	0.397383
	g_Z	18.832486	18.984133	18.679197	18.856638	18.338944	18.390529
2	g_X	0.427900	0.402825	0.455629	0.397776	2.407767	1.5689983
	g_Y	0.667345	0.489026	0.694601	0.495705	2.850576	2.6897113
	g_Z	17.114847	17.163176	16.866767	17.000860	14.502591	13.9767522
3	g_X	2.110386	0.226474	2.015303	0.291603	0.675701	1.311372
	g_Y	3.585327	1.196066	2.622207	0.869917	2.054387	2.040459
	g_Z	12.880713	14.725873	13.575522	15.006331	16.692948	15.104070
4	g_X	8.815301	2.720775	0.523589	3.046532	0.578700	0.444426
	g_Y	6.435000	6.627713	4.783768	6.852590	1.446302	0.911001
	g_Z	1.104218	11.859700	9.573178	11.500577	12.746527	13.759828